Desalination and Water Treatment
www.deswater.com
doi: 10.5004/dwt.2020.25150

192 (2020) 1–10
July

Comparison of aeration effect between pressure-driven and thermal membrane processes

Jihyeok Choi, Yongjun Choi, Jaehyun Ju, Bomin Kim, Youngkyu Park, Sangho Lee*

School of Civil and Environmental Engineering, Kookmin University, 77 Jeongneung-ro, Seoungbuk-gu, Seoul 02707, Korea, Tel./Fax: +82-2-910-4529; email: sanghlee@kookmin.ac.kr (S. Lee)

Received 1 July 2019; Accepted 18 November 2019

ABSTRACT

Microporous membranes have been widely used in various water treatment systems, including pressure-driven separation processes such as microfiltration (MF) and ultrafiltration (UF) and thermally-driven separation processes such as membrane distillation (MD). However, control of membrane fouling is key to the successful design and operation of these processes. In this study, the effect of aeration on the fouling control was investigated in MF and MD processes, which have different driving forces. Experiments were carried out using the same microporous membranes in MF and MD processes to compare the difference in fouling propensity and the antifouling effect by the aeration. The reversibility of the foulants deposited on the membrane was also compared. Hermia's fouling models were applied to analyze the aeration effect in both MF and MD but failed to fit the experimental data in most cases. Accordingly, a novel fouling model was suggested and used to interpret the experimental results. The specific fouling potential (ϕ) was introduced to show how the fouling potential changes during the operation of the membrane processes. It was confirmed from this analysis that the aeration effect was different between MF and MD, which is attributed to the inherent difference in the driving forces.

Keywords: Microfiltration; Membrane distillation; Fouling; Aeration; Model

1. Introduction

With the growth in water demand and water quality deterioration, the use of microfiltration membranes in water industries has become increasing important. A microporous membrane is defined as a structure having pores typically ranging from 0.03 to 10 μm in diameter. One of the usages of such membrane is microfiltration (MF), which is a pressure-drive process for water and wastewater treatment [1–3]. A typical configuration of MF is the cross-flow microfiltration (CFMF) where the feed solution flows along the membrane surface with only a small portion of the liquid passing through the membrane as a permeate [4]. The CFMF is preferably applied for the filtration of liquids with a high solids concentration [5]. Another usage of the microporous membrane is membrane distillation (MD), which is a thermally-driven separation process. The separation by MD is enabled due to phase change using hydrophobic membrane [6,7]. MD allows a very high rejection for ionic species in feed water and has the advantage of using renewable energy technology [8–10]. Accordingly, MD has been considered for seawater desalination and near-zero liquid discharge.

Nevertheless, membrane fouling is a common problem in processes using microporous membranes [11–14]. The occurrence of membrane fouling has been reported to be closely related to foulant properties such as surface energy [15]. Inorganic foulants were found to reduce the effective

* Corresponding author.

membrane area of the membrane, leading to a decrease in water production [16,17]. Since membrane fouling results in an increase in operation and maintenance cost of the process, its retardation or minimization of membrane fouling is important.

Accordingly, there have been a lot of studies on the control of fouling for microporous membranes. For example, Oh et al. [18] introduced the sequence of physical cleaning by changing cross-flow velocity. Zhang et al. [19] applied ultrasonic to control membrane fouling and enhance process performance. Racar et al. [20] compared chemical cleaning methods to remove membrane fouling. Although ultrasonic and chemical cleaning may be effective to remove foulants from the membrane, they may also damage membranes with excessive exposure. With this reason, aeration has been widely applied in practical membrane processes.

Understanding the fouling behaviors is also important for preventative management of membrane fouling. This has led to substantial amounts of study on the development of fouling models [21,22]. These fouling models may be also used to identify the dominant fouling mechanisms based on the model fit results. Unfortunately, relatively few works have been done to develop fouling models that can be applied not only to MF but also MD because of the inherence difference between the two processes.

In this study, the control of membrane fouling in MF and MD processes was attempted by applying an aeration technique. The same microporous membrane and foulants were used for both processes to understand their differences. The fouling patterns and the effectiveness of the aeration were theoretically analyzed using modeling approaches. Based on these results, a novel fouling model was derived and applied to provide in-depth information on fouling control in MF and MD processes. The novelty of this work lies on (1) the comparison of aeration effect in MF and MD using the same membrane and (2) the development of the fouling model that can be applied to both membrane processes.

2. Material and methods

2.1. Experimental materials and methods

A hydrophobic polyvinylidene fluoride (PVDF) flat sheet membrane supplied by Merck Millipore Ltd., (GVHP14250, U.S.A) was selected for the experiments. Since the membrane was hydrophobic, it was immersed into an alcohol solution for 30 min prior to MF experiments. The membrane parameters and relevant process conditions are listed in Table 1. The feed solution containing the colloidal silica (ST-ZL, SNOWTEX, Japan) of 5,000 mg/L was used for accelerated fouling testing. The experimental sets are summarized in Table 2.

2.2. Experimental set-up

Fig. 1 shows the experimental set-ups for MF (Fig. 1a) and MD (Fig. 1b). The size of the membrane module was the same. The feed flow rate was also adjusted to be same in both processes. The applied pressure for MF was 0.05 bar and the temperature difference between the feed and the permeate sides for MD was 40°C. The pressure was adjusted with a valve at the outlet of the module and the temperature of feed and permeate side were maintained constantly by a hot plate stirrer and water bath. The thermometers were used for measuring the inlet and outlet temperature of feed and permeate flow. The air pump was placed in front of the module to affect the membrane directly. The flow rates of air were fixed at 50 and 150 mL/min, respectively. The Reynolds number of the feed solution was 2,620, which indicates the laminar flow regime. During the aeration, the bubble size was measured at approximately 5.5–18 mm (Fig. 1c).

2.3. Theory

2.3.1. Hermia's fouling model

The blocking filtration models based on the Herima's model equations were used to fit the changes in flux with time. The fouling mechanism can be divided into three categories: pore blockage, pore constriction, and cake filtration. Table 3 summarizes Hermia's model equations and parameters. Here, A is the effective area of the membrane surface, α_{block} is the measure of the pore blockage efficiency, J_0 is the initial filtrate flux through the clean membrane and N_0 is the initial pore density. The variables were assigned to K and created a function for time. Each foulant identified a dominant mechanism for flux reduction by time.

Table 1
Summary of membrane parameters and process conditions

	Microfiltration (MF)	Membrane distillation (MD)
Membrane type	Flat sheet membrane	
Membrane material	Hydrophilic polyvinylidene fluoride (PVDF)	Hydrophobic polyvinylidene fluoride (PVDF)
Pore diameter (μm)	0.22	
Porosity (%)	75	
Effective area (cm^2)	12 (6 cm × 2 cm)	
Feed temperature	20	60
Permeate temperature	20	
Feed pressure (bar)	0.05	–
Feed velocity (cm/s)	14.58	

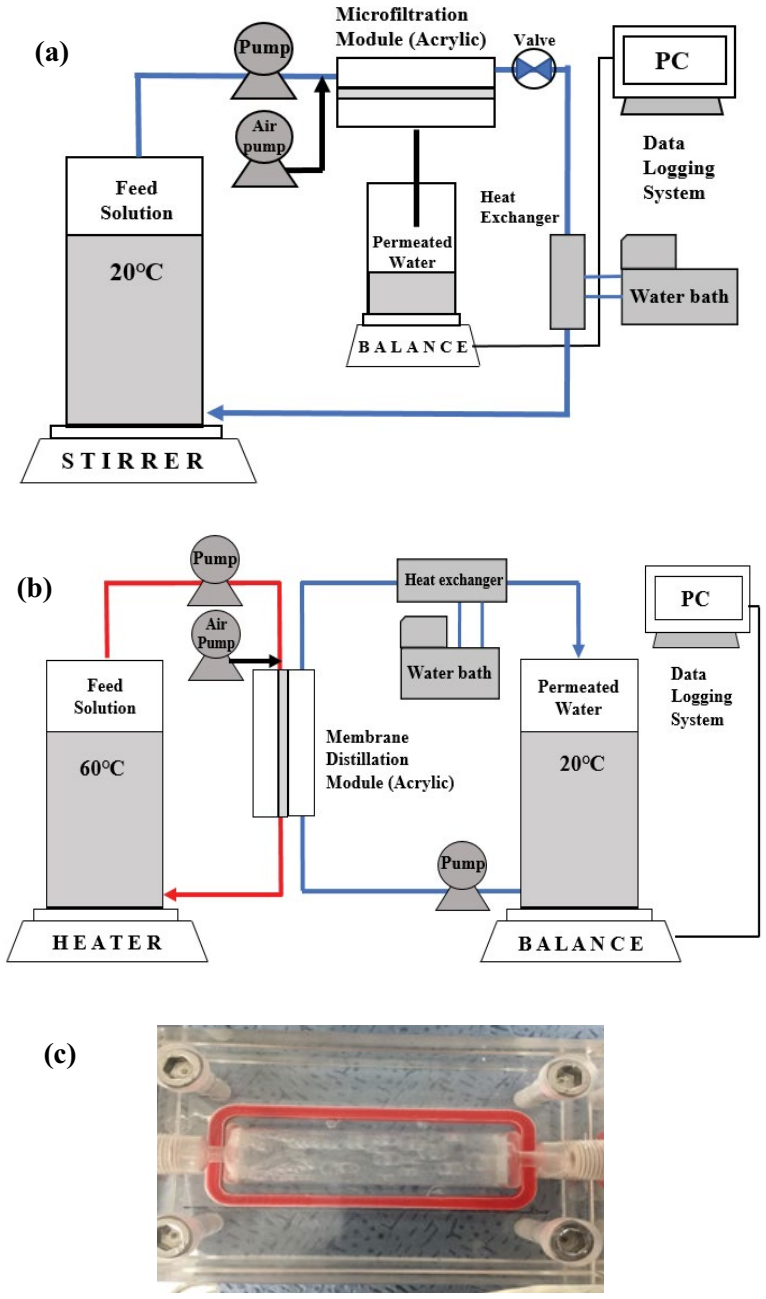

Fig. 1. Schematic diagram of laboratory-scale experimental set-up. (a) MF, (b) MD, and (c) photograph of air flowing inside the module.

Table 2
Summary of experimental case

Case		Microfiltration (MF)	Membrane distillation (MD)
1	2	Basic condition (non-aeration)	
3	4	Case 1,2 + Aeration 50 mL/min	
5	6	Case 1,2 + Aeration 150 mL/min	
7	8	Case 1,2 + Initial flux checked after flushing (15 min)	
9	10	Case 3,4 + Initial flux checked after flushing (15 min)	
11	12	Case 5,6 + Initial flux checked after flushing (15 min)	

Table 3
Three typical Hermia's fouling model

Filtration model	Model equation	Model parameter
Pore blockage	$\frac{J_v}{J_o}=\exp\left(-\frac{\alpha_{block}AJ_oC_b}{N_o}t\right)$	$Kt=\ln\left(\frac{J_o}{J_v}\right)$
Pore construction	$\frac{J_v}{J_o}=\left(1+\frac{\alpha_{pore}AJ_oC_b}{\pi r_o^2\delta_m}t\right)^{-2}$	$Kt=\left(\frac{J_o}{J_v}\right)^{1/2}-1$
Cake filtration	$\frac{J_v}{J_o}=\left(1+\frac{2\alpha_{cake}J_oC_b}{R_m}t\right)^{-\frac{1}{2}}$	$Kt=\left(\frac{J_o}{J_v}\right)^{2}-1$

2.3.2. Model derivation

In addition to Hermia's model, the following model equation was derived for both MF and MD processes. The flux both processes was calculated by the following flux equations:

$$J_{MF}=\frac{\Delta P}{\mu R_t} \tag{1}$$

$$R_t=R_m+R_f \tag{2}$$

where J is the MF flux and ΔP is the transmembrane pressure, μ is the viscosity, R_t is the total resistance, R_m is the membrane resistance, and R_f is the fouling resistance.

$$J_{MD}=B\Delta P_{vap} \tag{3}$$

where J_w is the MD flux and B is the membrane coefficient (the membrane permeability). ΔP_{vap} is the transmembrane pressure difference of water vapor, and the water vapor pressure calculated by the Antoine equation is 0.175.

The fouling resistance may be assumed to be linearly proportional to the amount of foulant deposited on the membrane surface. Using this assumption, the following equations can be obtained for MF.

$$J_{MF}=\frac{\Delta P}{\mu R_t}=\frac{\Delta P}{\mu\left(R_m+R_f\right)} \tag{4}$$

$$R_f=\frac{m_d}{A}\times\phi=\frac{\phi C_bV_p}{A}=\frac{\phi C_bJ_{MF}At}{A}=\phi C_bJ_{MF}t \tag{5}$$

$$J_{MF}=\frac{\Delta P}{\mu\left(R_m+\phi C_bJ_{MF}t\right)} \tag{6}$$

$$\phi=\frac{\frac{\Delta P}{\mu J_{MF}}-R_m}{C_bJ_{MF}t} \tag{7}$$

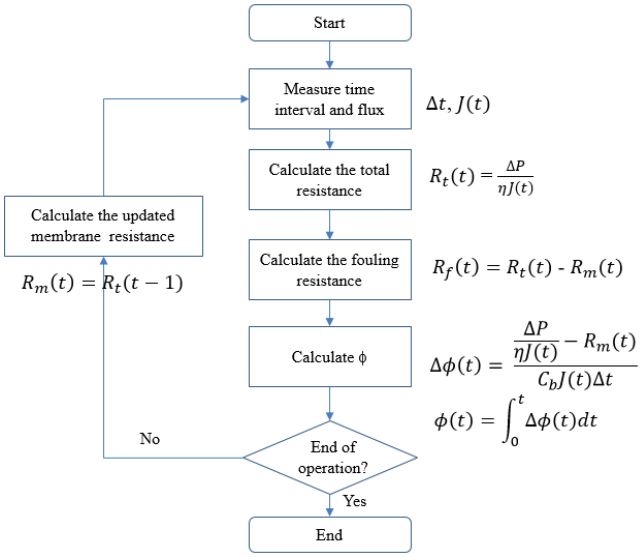

Fig. 2. Algorithm of the modeling approach.

where m_d is the amount of the foulant, A is the membrane area, and ϕ is the specific fouling potential. Similarly, the following equations can be obtained for MD.

$$J_{MD}=B\Delta P_{vap}=\frac{\Delta P_{vap}}{\frac{1}{B_{new}}+\mu R_f}=\frac{\Delta P_{vap}}{1/B_{new}+\mu\phi C_bJ_{MD}t} \tag{8}$$

$$\phi=\frac{\frac{\Delta P_{vap}}{J_{MD}}-\frac{1}{B_{new}}}{\mu C_bJ_{MD}t} \tag{9}$$

where B_{new} is a permeability coefficient for a new membrane, the ϕ value can be also calculated in MD through Eq. (9). The ϕ value is a measure of the possibility of contamination per unit mass of foulants. It is proportional to the contamination possibility and resistance value.

2.3.3. Modeling approach

As shown in Fig. 2, the model algorithm to calculate the ϕ value by time. After measuring the flux on time, the R_t value is calculated. The R_f value was obtained from the calculated R_t value. After obtaining the ϕ value through the deduced equation, model fitting was performed by updating the R_m value. In both processes, the values of ϕ with and without aeration were compared.

3. Results and discussions

3.1. Comparison of fouling propensity in MF and MD

To begin, the fouling behaviors of the microporous membranes in MF and MD were examined without applying the aeration. In Fig. 3a the flux was initially high in the MF process but rapidly decreased to reach a steady-state flux after 30 min. On the other hand, the flux gradually

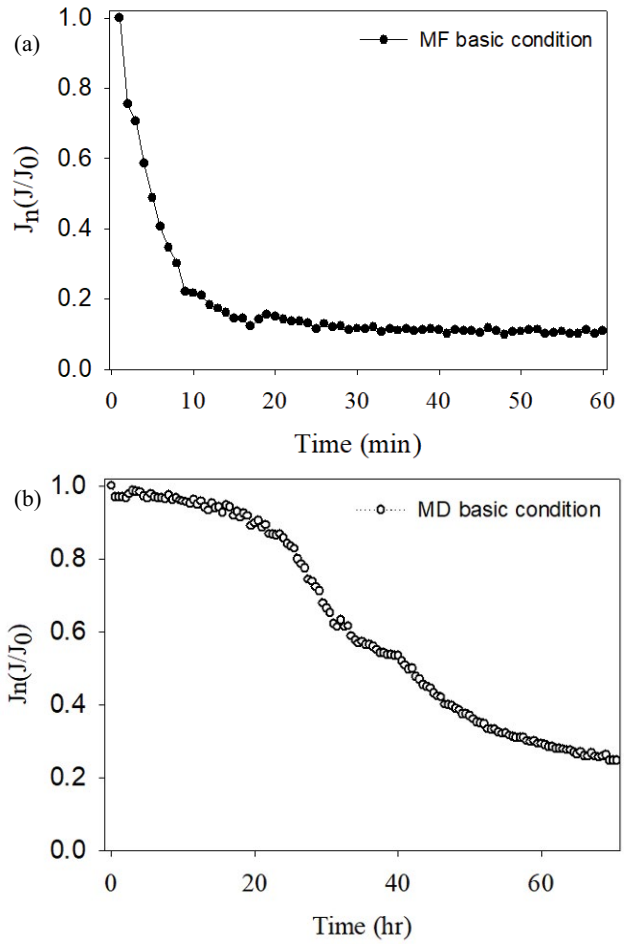

Fig. 3. Comparison of fouling propensity in basic condition, (a) MF and (b) MD.

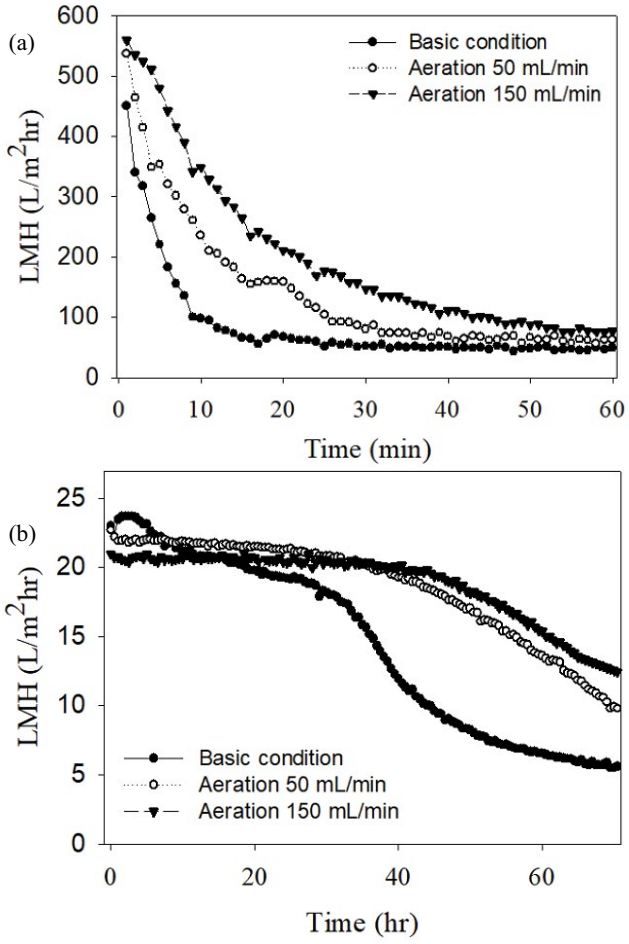

Fig. 4. Effect of aeration each case in (a) MF and (b) MD.

decreased in the MD process. This is attributed to the difference in the driving force between MF and MD processes. In the MF process, the driving force is the hydraulic pressure, which induces compaction of the foulants on the membrane surface. As a result, fouling can be accelerated. In the MD process, however, the driving force is the vapor pressure difference caused by the temperature difference. Accordingly, there is no hydraulic pressure onto the foulant layer. Moreover, the initial flux values for MF (–500 L/m² h) and MD (–23 L/m² h) processes was also different, thereby affecting the fouling behaviors.

3.2. Effect of aeration and flushing

A set of experiments were carried out to investigate the effect of aeration on fouling in MF and MD. The aeration rates were 50 and 150 mL/min, respectively. As shown in Fig. 4a, the initial flux in MF increased by 20%–25% with the application of the aeration. The rate of flux decline in the initial phase of the filtration was also reduced but the final flux at 60 min was similar. On the other hand, the aeration seems to be more effective to control fouling in MD than in MF, as demonstrated in Fig. 4b. After 30 min, the difference in flux between the runs without and with aeration became significant. The final flux at 60 min was also higher with the aeration than without the aeration. This suggests that the aeration can be successfully applied to control fouling in MD.

Fig. 5a compares the fouling resistances in the MF process. As the aeration intensity increases, the fouling resistance decreases, which supports the results in Fig. 4a. The initial and final flux values in MD were compared in Fig. 5b. Again, the aeration appears to increase the final flux by more than two times with the application of the aeration at 150 mL/min.

The effect of aeration on the flushing efficiency was also examined in both MF and MD. After each experiment was completed, the flux was measured after the flushing of 15 min. The R_t value was directly calculated from the flux and the R_f value was also obtained. Then, the flushing efficiency (f) value was estimated as:

$$\text{Flusing efficiency}\left(f\right)=\frac{R_f-R_{f'}}{R_f}\times 100\left(\%\right) \tag{10}$$

where $R_{f'}$ is the fouling resistance and R_f is the fouling resistance after flushing. As shown in Fig. 6a the f value

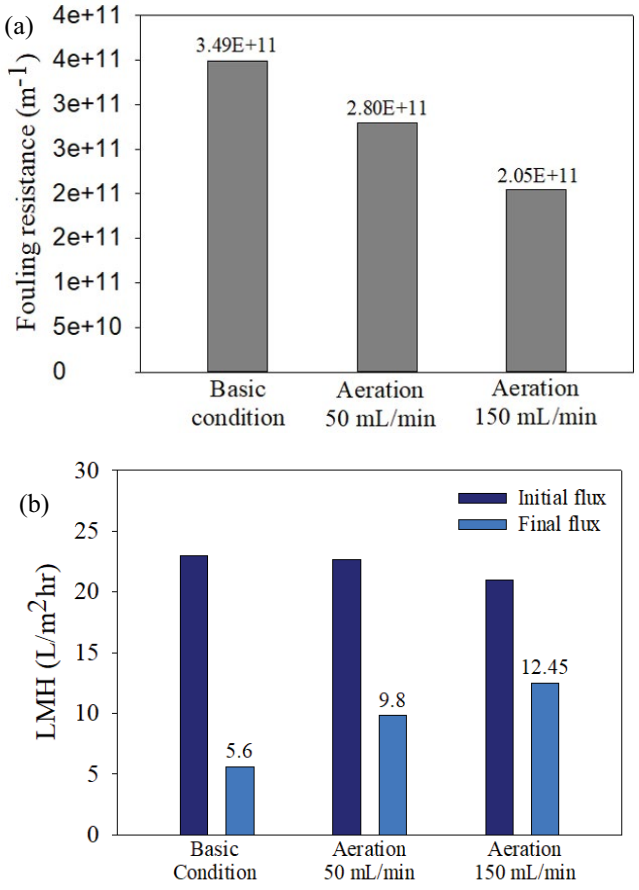

Fig. 5. (a) Comparison of fouling resistance value in MF and (b) comparison of initial and final flux in MD.

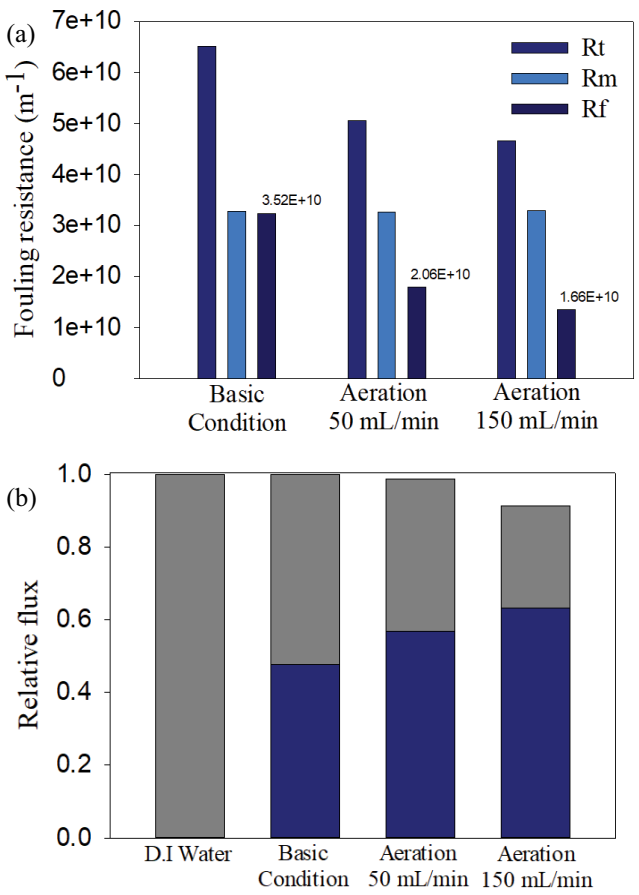

Fig. 6. Effect of aeration on flushing efficiency. (a) Comparison of total resistance value ($R_t = R_m + R_f$) in MF and (b) comparison of permeability in MD.

was 41% and 82%, which improved the cleaning efficiency. In Fig. 6b, the relative initial flux increased with the addition of aeration and the recovery rate improved up to 18%. In summary, it appears that the aeration enhances the flushing efficiency by making the foulant layer more reversible.

3.3. Fouling model

3.3.1. Hermia's model fit

The conventional fouling model (Hermia's model) was applied to fit the flux data and identify the major fouling mechanisms. Unfortunately, the model fits were not successful to fit the experimental results in both MF and MD as shown in Figs. 7 and 8. Except for Fig. 7f, the R^2 values were too low to be used for further interpretation. It seems that more than two fouling mechanisms were involved in the fouling, which failed the reasonable model fits by the Herima's model.

3.3.2. Model for the analysis of specific fouling potential

As an alternative to Hermia's model, the model derived from section 2.3.2 (model derivation) was applied to interpret the fouling behavior on the membrane surface due to the presence of the aeration. The information that can be obtained from this model analysis the changes in the specific fouling potential (ϕ) with time, allowing an in-depth analysis of fouling propensity under different conditions. Fig. 9a shows the dependence of ϕ on time in the basic condition (without aeration) and with the aeration in the MF process. The ϕ value rapidly increased in the beginning and then gradually decreased when there was no aeration. However, the rapid increase in ϕ at the initial phase was not observed when the aeration was applied. This suggests that the aeration was effective to suppress the initial fouling in MF by affecting the fouling potential.

In Fig. 9b, the changes in ϕ were shown with time in the basic condition and with the aeration in the MD process. Unlike MF, there was no rapid increase in ϕ in the initial period of time. Instead, ϕ began to increase after 20 min without the aeration. When the aeration was applied, the increase in ϕ with time was significantly reduced. It is evident that the probability of the foulant deposition and attachment on to membrane surface in the MD process decreased by introducing the aeration, which was effective to suppress the fouling occurred after a certain period of time.

Using the results in Fig. 9, box plots were made to visualize the statistical information on the data. Without the aeration in MF (Fig. 10a), the mean and standard deviation of the data was high, indicating the widespread distribution

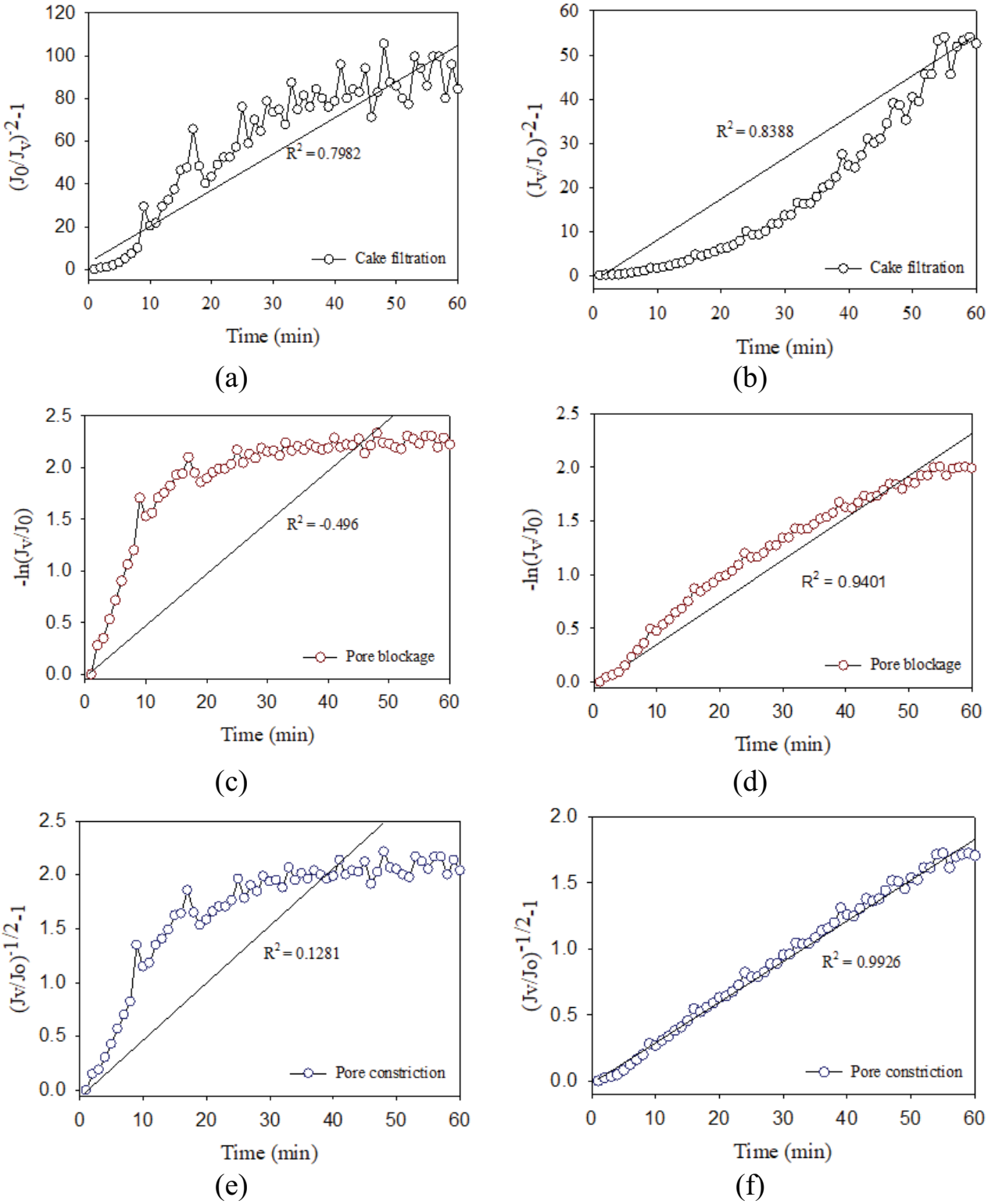

Fig. 7. Hermia's fouling model fitting in MF. (a) Pore blocking, without aeration, (b) pore constriction, without aeration, (c) cake formation, without aeration, (d) pore blocking, aeration at 150 mL/min, (e) pore constriction, aeration at 150 mL/min, and (f) cake formation, aeration at 150 mL/min.

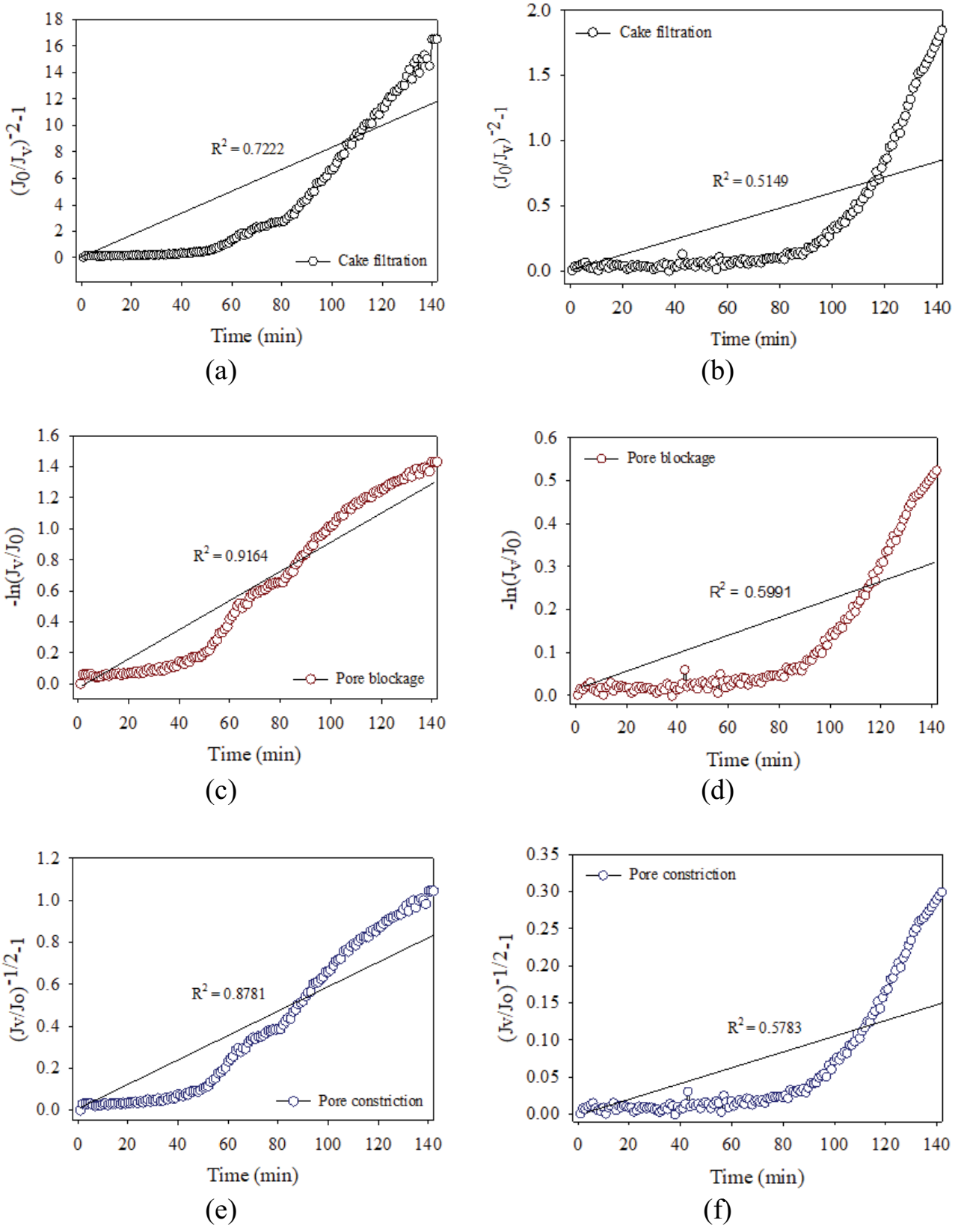

Fig. 8. Hermia's fouling model fitting in MD. (a) Pore blocking, without aeration, (b) pore constriction, without aeration, (c) cake formation, without aeration, (d) pore blocking, aeration at 150 mL/min, (e) pore constriction, aeration at 150 mL/min, and (f) cake formation, aeration at 150 mL/min.

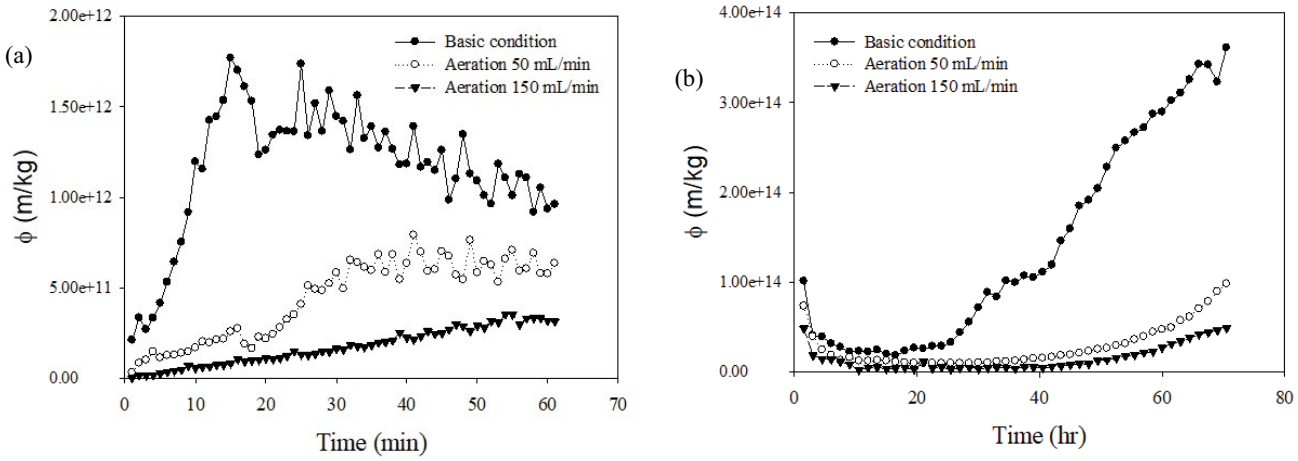

Fig. 9. Calculation of ϕ in MF and MD (a) MF and (b) MD.

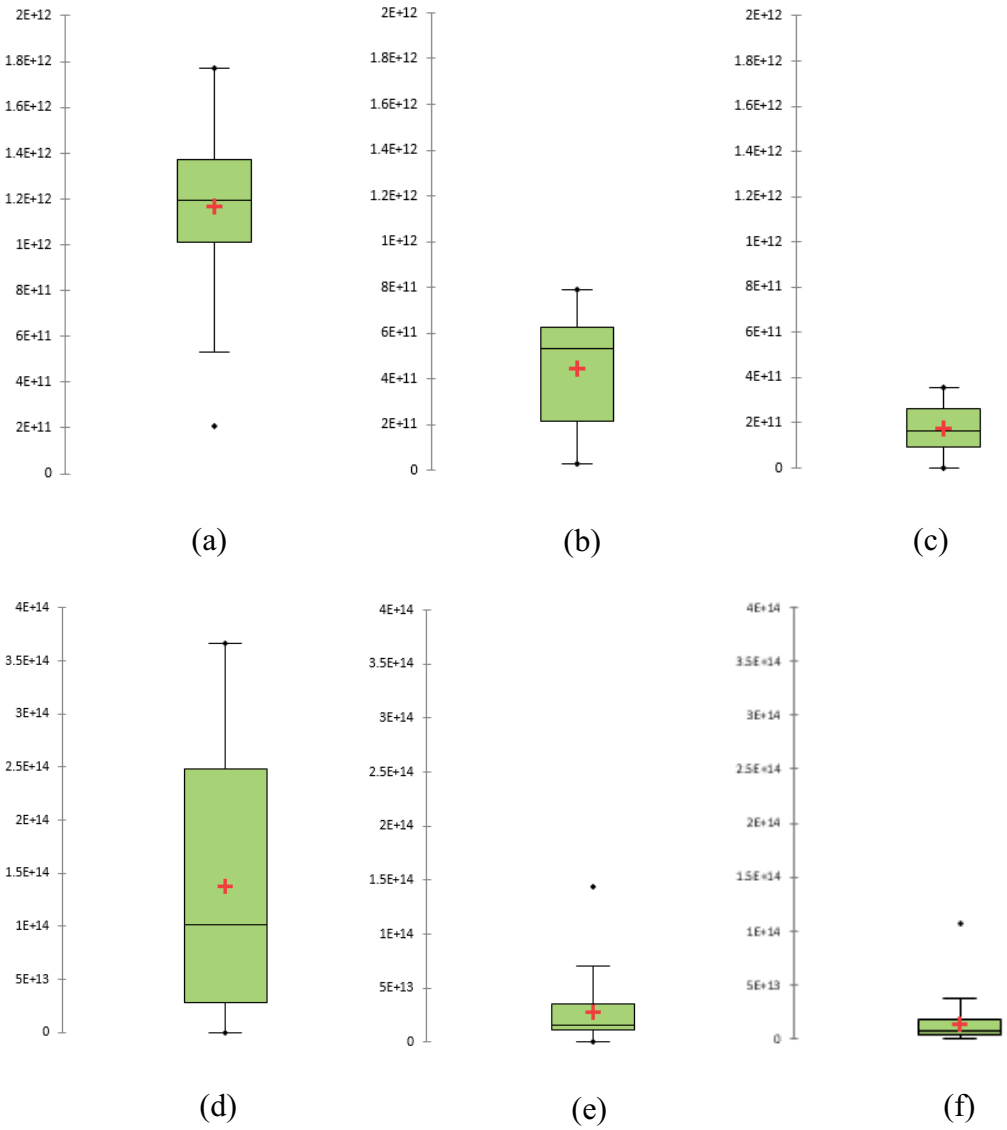

Fig. 10. Calculation of ϕ in MF and MD using box plot. (a) MF without aeration, (b) MF with aeration at 50 mL/min, (c) MF with aeration at 150 mL/min, (d) MD without aeration, (e) MD with aeration at 50 mL/min, and (f) MD with aeration at 150 mL/min.

of ϕ. By applying the aeration in MF (Figs. 10b and c), both mean and standard deviation were reduced, indicating that the performance became more stable. Similar results were observed in MD, as indicated in Figs. 10d–f. But it also seems that the effect of the aeration on the mean and standard deviation of ϕ was greater in MD than in MF.

4. Conclusions

In this work, the effect of aeration on the control of fouling caused by the colloidal silica was investigated in MF and MD processes. The following conclusions were withdrawn:

- Although these experiments were used under the same membrane and similar hydrodynamic condition, the fouling propensity in MF was higher than that in MD. This is probably because of the difference in the hydraulic pressure and the initial flux.
- As expected, the application of aeration reduced the fouling in both MF and MD. Aeration also affected the flushing efficiency, suggesting that the foulant properties may be altered by aeration.
- Hermia's model fit was not applicable to explain the fouling mechanisms. Accordingly, a new model was suggested to analyze the fouling behaviors without and with aeration. In both MF and MD, the aeration was found to significantly reduce the specific fouling potential (ϕ). The aeration was more effective to decrease the fouling potential in MD than in MF. By applying the aeration in MF and MD, both mean and standard deviation for ϕ were reduced, indicating that the membrane performance became more stable.

Acknowledgment

This subject is supported by Korea Ministry of Environment as "Global Top Project (2017002100001)."

References

[1] A. Hoque, K. Kimura, T. Miyoshi, N. Yamato, Y. Watanabe, Characteristics of foulants in air-sparged side-stream tubular membranes used in a municipal wastewater membrane bioreactor, Sep. Purif. Technol., 93 (2012) 83–91.
[2] A. Echavarría, C. Torras, J. Pagán, A. Ibarz, Fruit juice processing and membrane technology application, Food Eng. Rev., 3 (2011) 136–158.
[3] K.V. Kotsanopoulos, I.S. Arvanitoyannis, Membrane processing technology in the food industry: food processing, wastewater treatment, and effects on physical, microbiological, organoleptic, and nutritional properties of foods, Crit. Rev. Food Sci. Nutr., 55 (2015) 1147–1175.
[4] K. Yu, X. Wen, Q. Bu, H. Xia, Critical flux enhancements with air sparging in axial hollow fibers cross-flow microfiltration of biologically treated wastewater, J. Membr. Sci., 224 (2003) 69–79.
[5] R. Makabe, K. Akamatsu, S.-i. Nakao, Mitigation of particle deposition onto membrane surface in cross-flow microfiltration under high flow rate, Sep. Purif. Technol., 160 (2016) 98–105.
[6] A. Alkhudhiri, N. Darwish, N. Hilal, Membrane distillation: a comprehensive review, Desalination, 287 (2012) 2–18.
[7] A. Ali, R.A. Tufa, F. Macedonio, E. Curcio, E. Drioli, Membrane technology in renewable-energy-driven desalination, Renewable Sustainable Energy Rev., 81 (2018) 1–21.
[8] G. Naidu, S. Jeong, Y. Choi, S. Vigneswaran, Membrane distillation for wastewater reverse osmosis concentrate treatment with water reuse potential, J. Membr. Sci., 524 (2017) 565–575.
[9] D. González, J. Amigo, F. Suárez, Membrane distillation: perspectives for sustainable and improved desalination, Renewable Sustainable Energy Rev., 80 (2017) 238–259.
[10] P. Wang, T.-S. Chung, Recent advances in membrane distillation processes: membrane development, configuration design and application exploring, J. Membr. Sci., 474 (2015) 39–56.
[11] R. Kumar, A. Ismail, Fouling control on microfiltration/ultrafiltration membranes: effects of morphology, hydrophilicity, and charge, J. Appl. Polym. Sci., 132 (2015) 42042.
[12] W. Zhang, L. Ding, Investigation of membrane fouling mechanisms using blocking models in the case of shear-enhanced ultrafiltration, Sep. Purif. Technol., 141 (2015) 160–169.
[13] W. Qin, Z. Xie, D. Ng, Y. Ye, X. Ji, S. Gray, J. Zhang, Comparison of colloidal silica involved fouling behavior in three membrane distillation configurations using PTFE membrane, Water Res., 130 (2018) 343–352.
[14] J. Gilron, Y. Ladizansky, E. Korin, Silica fouling in direct contact membrane distillation, Ind. Eng. Chem. Res., 52 (2013) 10521–10529.
[15] F. Zamani, A. Ullah, E. Akhondi, H.J. Tanudjaja, E.R. Cornelissen, A. Honciuc, A.G. Fane, J.W. Chew, Impact of the surface energy of particulate foulants on membrane fouling, J. Membr. Sci., 510 (2016) 101–111.
[16] D.M. Warsinger, J. Swaminathan, E. Guillen-Burrieza, H.A. Arafat, Scaling and fouling in membrane distillation for desalination applications: a review, Desalination, 356 (2015) 294–313.
[17] S. Shirazi, C.-J. Lin, D. Chen, Inorganic fouling of pressure-driven membrane processes—a critical review, Desalination, 250 (2010) 236–248.
[18] H. Oh, J. Eom, S. Kang, B. Lee, H. Yoo, B. Lee, A study on enhancing physical cleaning effectiveness in microfiltration membrane system, Desal. Water Treat., 54 (2015) 3596–3602.
[19] R. Zhang, Y. Huang, C. Sun, L. Xiaozhen, X. Bentian, Z. Wang, Study on ultrasonic techniques for enhancing the separation process of membrane, Ultrason. Sonochem., 55 (2019) 341–347.
[20] M. Racar, D. Dolar, K. Košutić, Chemical cleaning of flat sheet ultrafiltration membranes fouled by effluent organic matter, Sep. Purif. Technol., 188 (2017) 140–146.
[21] M.-J. Corbatón-Báguena, S. Álvarez-Blanco, M.-C. Vincent-Vela, Fouling mechanisms of ultrafiltration membranes fouled with whey model solutions, Desalination, 360 (2015) 87–96.
[22] H. Esfahani, M.P. Prabhakaran, E. Salahi, A. Tayebifard, M.R. Rahimipour, M. Keyanpour-Rad, S. Ramakrishna, Electrospun nylon 6/zinc doped hydroxyapatite membrane for protein separation: mechanism of fouling and blocking model, Mater. Sci. Eng., C, 59 (2016) 420–428.